

This article appeared in a journal published by Elsevier. The attached copy is furnished to the author for internal non-commercial research and education use, including for instruction at the authors institution and sharing with colleagues.

Other uses, including reproduction and distribution, or selling or licensing copies, or posting to personal, institutional or third party websites are prohibited.

In most cases authors are permitted to post their version of the article (e.g. in Word or Tex form) to their personal website or institutional repository. Authors requiring further information regarding Elsevier's archiving and manuscript policies are encouraged to visit:

<http://www.elsevier.com/copyright>



Contents lists available at ScienceDirect

Electrochimica Acta

journal homepage: [www.elsevier.com/locate/electacta](http://www.elsevier.com/locate/electacta)

# Polyaniline Langmuir–Blodgett film modified glassy carbon electrode as a voltammetric sensor for determination of $\text{Ag}^+$ ions

Qiongyan Liu<sup>a</sup>, Fei Wang<sup>a,b</sup>, Yonghui Qiao<sup>a</sup>, Shusheng Zhang<sup>a</sup>, Baoxian Ye<sup>a,\*</sup>

<sup>a</sup> Department of Chemistry, Zhengzhou University, Zhengzhou, 450001, China

<sup>b</sup> Department of Material and Chemistry Engineering, Henan Institute of Engineering, Zhengzhou, 450007, China

## ARTICLE INFO

### Article history:

Received 30 July 2009

Received in revised form 27 October 2009

Accepted 27 October 2009

Available online 1 November 2009

### Keywords:

Langmuir–Blodgett film

Polyaniline

p-Toluenesulfonic acid

Voltammetric sensor

Silver (I) ion

## ABSTRACT

A highly sensitive electrochemical sensor made of a glassy carbon electrode (GCE) coated with a Langmuir–Blodgett film (LB) containing polyaniline (PAn) doped with p-toluenesulfonic acid (PTSA) (LB/PAn-PTSA/GCE) has been used for the detection of trace concentrations of  $\text{Ag}^+$ . UV–vis absorption spectra indicated that the PAn was doped by PTSA. The surface morphology of the PAn LB film was characterized by atomic force microscopy (AFM). The electrochemical properties of this LB/PAn-PTSA/GCE were studied using electrochemical impedance spectroscopy (EIS) and cyclic voltammetry. The LB/PAn-PTSA/GCE was used as a voltammetric sensor for determination of trace  $\text{Ag}^+$  at pH 5.0 using linear scanning stripping voltammetry. Under the optimal experimental conditions, the stripping current was proportional to the  $\text{Ag}^+$  concentration over the range from  $6.0 \times 10^{-10} \text{ mol L}^{-1}$  to  $1.0 \times 10^{-6} \text{ mol L}^{-1}$ , with a detection limit of  $4.0 \times 10^{-10} \text{ mol L}^{-1}$ . The high sensitivity, selectivity, and stability of this LB/PAn-PTSA/GCE also demonstrated its practical utility for simple, rapid and economical determination of  $\text{Ag}^+$  in water samples.

© 2009 Elsevier Ltd. All rights reserved.

## 1. Introduction

Conducting polymers consisting of conjugated electronic structures such as polypyrrole, polythiophene, or polyaniline have received considerable attention lately because of their many promising uses. Polyaniline is an environmentally stable and technologically important conducting polymer whose electronic conductivity can be reversibly altered by both oxidation/reduction and acid/base chemistries [1]. Polyaniline can exist as “salts” or “bases” in three isolable oxidation states: leucoemeraldine (LES or LEB), emeraldine (ES or EB), and pernigraniline (PS or PB). Among these three states, only the emeraldine salt (ES) is electrically conductive [2]. Polyaniline membranes have been widely utilized as chemical sensors, including biomolecular sensors [3–9], ammonia sensors [10], small organic molecule sensors [11,12], hydrogen sensors [13,14] and inorganic ion sensors [15–17]. However polyaniline and polyaniline membranes are not widely used as sensors for inorganic ions such as noble metals. In particular, polyaniline membranes are rarely if ever used for detection of  $\text{Ag}^+$  ions. Recently Evtugyn et al. [18,19] fabricated polyaniline and thiacalix[4]arene derivatized composite membranes on glassy carbon and employed the sensors for potentiometric determination of  $\text{Ag}^+$ . The modified electrodes were obtained by initially depositing polyaniline using electropolymerization, and subsequently placing thiacalix[4]arene onto the electrode.

bon and employed the sensors for potentiometric determination of  $\text{Ag}^+$ . The modified electrodes were obtained by initially depositing polyaniline using electropolymerization, and subsequently placing thiacalix[4]arene onto the electrode.

Anodic stripping voltammetry (ASV) is a well-known analytical technique which is suitable for determination of trace metals due to its remarkable sensitivity, experimental simplicity, low equipment and maintenance costs, and low sample pretreatment requirements. Conventional mercury electrodes (hanging mercury electrode and mercury film electrode) have historically been widely used in ASV. However, due to its toxicity, mercury electrodes are generally avoided nowadays. Consequently, various mercury-free electrodes have been considered for sensitive determination of metals. A great deal of interest has recently been devoted to electrodes modified by LB films. LB films are considered to be more suitable for the fabrication of modified electrodes, as the ordered arrangement of molecules and the nano-scale film thickness are likely to allow both high sensitivity and ultrafast response times [20]. Manigandan et al. [21] have produced nanostructured polyaniline using the Langmuir–Blodgett technique, and have used their substrate as an ammonia sensor. As far as we are aware, GC electrode modified by a LB film of polyaniline has never before been used for voltammetric sensing of  $\text{Ag}^+$ .

In this paper, a novel voltammetric sensor based on a GC electrode modified with a polyaniline LB film doped by p-toluenesulfonic acid (PTSA) was prepared and successfully used for

\* Corresponding author at: Department of Chemistry, Zhengzhou University, Zhengzhou, China. Tel.: +86 0371 67781757; fax: +86 0371 67763654.

E-mail address: [yebx@zzu.edu.cn](mailto:yebx@zzu.edu.cn) (B. Ye).

determination of trace  $\text{Ag}^+$ . The aim of this work is to establish a simple, environmentally friendly, and sensitive method for determination of trace  $\text{Ag}^+$  in water samples. The experimental results show that the established method possesses high sensitivity, good reproducibility, a broad dynamic range ( $6.0 \times 10^{-10} \text{ mol L}^{-1}$  to  $1.0 \times 10^{-6} \text{ mol L}^{-1}$ ) and a low detection limit ( $4.0 \times 10^{-10} \text{ mol L}^{-1}$ ).

## 2. Experimental

### 2.1. Apparatus and reagents

The electrochemical measurements were performed using RST3000 (Zhengzhou Shiruisi Instrument Technology Co., Ltd, China) and CHI650 (CH Instruments Company, USA) electrochemical analyzers. LB films were formed and deposited on a GCE using JML-04 LB trough (Shanghai Zhongchen Company, China). A traditional three-electrode system consisting of a saturated calomel reference electrode (SCE), a platinum auxiliary electrode, and the GC working electrode modified with a polyaniline/p-toluenesulfonic acid LB film ( $\phi$ , 3 mm) was employed. A monocrystalline silicon wafer was also used as a substrate when preparing LB films for examination by atomic force microscopy. The UV-vis spectra were recorded with a Model UV-2102PC spectrophotometer (UNICO, Shanghai, China). A Model 5500 atomic force microscope (Agilent, United States) was used to study the surface morphology of the LB films.

All reagents were analytical grade and were used without further purification. The aqueous solutions were prepared with re-distilled water. Methanol was used as the solvent when doping the polyaniline (PAn) emeraldine base (Sigma Aldrich; Mw ca. 10,000) with p-toluenesulfonic acid (PTSA) to produce the PAn-PTSA [21]. A stock solution of  $1.0 \times 10^{-3} \text{ mol L}^{-1} \text{ AgNO}_3$  was prepared with re-distilled water and stored in the dark. The  $\text{Ag}^+$  standard solutions were prepared daily by dilution of the stock solution.

### 2.2. Preparation of PAn-PTSA LB films

The PAn LB films were transferred both to the GC disk electrode for  $\text{Ag}^+$  determination and to the monocrystalline silicon wafer for characterization. The GC electrode was pretreated according to the normal method before coating, then electrochemically pretreated by cycling the electrode between  $\pm 1 \text{ V}$  in  $0.5 \text{ mol L}^{-1} \text{ H}_2\text{SO}_4$  until a stable CV curve was obtained. A sample of PAn-PTSA was spread on a p-toluenesulfonic acid aqueous solution subphase (pH 1.5). A Wilhelmy balance was used as the surface pressure sensor, and was situated in the middle of the trough. The monolayer was compressed at a rate of  $10 \text{ mm min}^{-1}$  after solvent evaporation, then was transferred onto the substrates (GC electrode or monocrystalline silicon wafer) at a rate of  $2.5 \text{ mm min}^{-1}$  under a surface pressure of  $15 \text{ mN m}^{-1}$  (vertical dipping). Z-type monolayer film deposition of PAn-PTSA on a cleaned silicon wafer and a clean, freshly pretreated electrode were achieved. The modified electrode was labeled "LB/PAn-PTSA/GCE." The multilayer films were assembled by sequential monolayer transfer.

### 2.3. Procedure

For determination of  $\text{Ag}^+$ ,  $0.2 \text{ mol L}^{-1} \text{ KNO}_3$  solution (pH 5.0) was employed as the supporting electrolyte. The accumulation of  $\text{Ag}^+$  proceeded for 200 s at  $-0.56 \text{ V}$  under stirring. The linear scanning stripping voltammetry measurement was performed from 0 V to  $0.5 \text{ V}$  (vs. SCE) at a scan rate of  $50 \text{ mV s}^{-1}$ . After that, the electrode was cleaned at  $0.3 \text{ V}$  for 60 s in a  $0.2 \text{ mol L}^{-1} \text{ KNO}_3$  blank solution (pH 5.0) to eliminate memory effects.

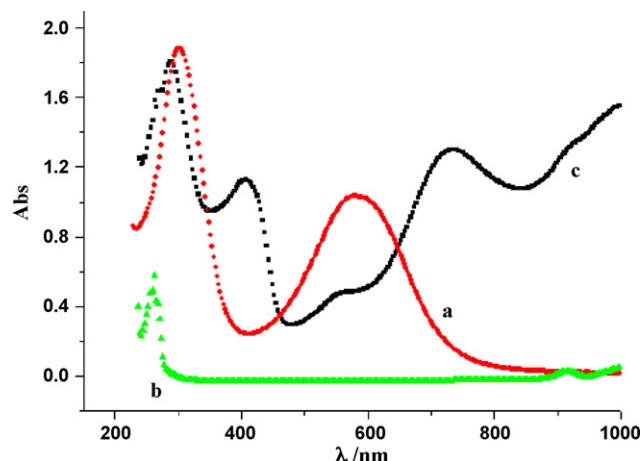


Fig. 1. UV-vis spectra of PAn (a), PTSA (b), and PAn-PTSA (c) in methanol solution.

## 3. Results and discussion

### 3.1. UV-vis spectra studies of PAn and PAn-PTSA in methanol solution

The UV-vis spectra of PAn, PTSA, and PAn-PTSA (Fig. 1a–c respectively) in methanol solution were studied to confirm the doping of PAn with PTSA. As shown in Fig. 1a for PAn, the characteristic absorption bands at 300 nm and 600 nm were attributed to the  $\pi-\pi^*$  transition of the benzene ring and the quinoid ring, respectively. The PTSA has no characteristic absorption in the wavelength range from 300 nm to 900 nm (Fig. 1b). When PAn was doped with PTSA, the characteristic absorption bands of PAn were red-shifted to 410 nm and 730 nm, respectively (Fig. 1c). Such behavior was due to changes in the molecular configuration of PAn. The doping of PAn by organic functional sulfonic acid changed the molecular configuration, which affected the electronic band structure and optical properties. When doped by larger size doping, the intermolecular force of PAn decreased and PAn took on an extended chain conformation. This extended conformation allowed charge delocalization and reduced the energy of the electronic absorption band. As a result, the spectrum red-shifted [22]. These spectral changes indicate that PAn was doped with PTSA [23].

### 3.2. The $\pi-A$ isotherm and structural characterization of PAn-PTSA LB films

Fig. 2 shows surface pressure isotherms of PAn-PTSA on a pH 1.5 subphase (a), and on a pH 1.5 subphase containing  $1.0 \times 10^{-4} \text{ mol L}^{-1} \text{ Ag}^+$  (b). As can be seen from curve a, the surface pressure was low at a relatively high area per molecule. Further compression produced a continuous rise in the isotherm. The collapse pressure was  $41.1 \text{ mN m}^{-1}$ , and the limiting area per molecule in the condensed state was  $1.13 \text{ nm}^2$  (obtained by extrapolating the linear part of the isotherm to  $\pi = 0$ ). Obviously, the isotherms suggested that PAn-PTSA formed a stable monolayer on the subphase surface. On the other hand, if the pH 1.5 subphase contained  $1.0 \times 10^{-4} \text{ mol L}^{-1} \text{ Ag}^+$ , a different isotherm was observed (Fig. 2b). This change implied that PAn could coordinate with  $\text{Ag}^+$  ions to form a monolayer at the air–water interface.

### 3.3. Structural characterization of PAn-PTSA LB film

Atomic force microscopy (AFM) imaging provides detailed information about the surface morphology of silicon modified with PAn-PTSA. The silicon substrates were successively sonicated in

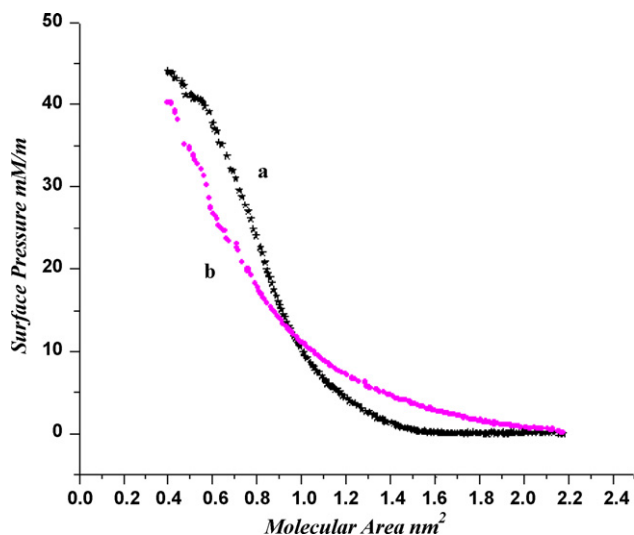


Fig. 2.  $\pi$ -A isotherms of PAN on (a) pH=1.5 and (b) pH=1.5 containing  $1.0 \times 10^{-4} \text{ mol L}^{-1} \text{ Ag}^+$  subphase.

ethanol and re-distilled water, each for 10 min. Then the substrates were dipped in piranha solution (the mixture of  $\text{H}_2\text{O}_2$  and  $\text{H}_2\text{SO}_4$  with a volume/volume ratio of 1:3) for 20 min. Finally, they were ultrasonically cleaned in re-distilled water for 5 min again and kept in re-distilled water for further use. Fig. 3 shows typical contact mode AFM images of the bare silicon surface (A) and of silicon covered with a layer of PAN-PTSA LB film (B) that was transferred from the air–water interface to the silicon surface under surface pressure of  $15 \text{ mN m}^{-1}$ . The bare silicon has no impurities on its surface, and shows a very even surface. The PAN-PTSA LB film was evenly distributed onto the surface of the silicon wafer. The average size (roughness) of the PAN-PTSA film was 207 nm.

### 3.4. Electrochemical impedance spectroscopy and cyclic voltammetry characterization of LB/PAN-PTSA/GCE

It is well known that electrochemical impedance spectroscopy (EIS) is an effective tool for studying the interface properties of surface-modified electrodes.  $R_{\text{et}}$ , the semicircle diameter at higher

frequencies in the Nyquist plot of EIS, can be used to describe the interface properties of the electrode because it controls interface electron transfer rate of the redox probe between the solution and the electrode. Its value varies when different substances are absorbed on the electrode [24]. Fig. 4 shows the results of EIS of a bare GCE and of different layers of a LB/PAN-PTSA/GC electrode in a solution containing  $1.0 \times 10^{-3} \text{ mol L}^{-1} \text{ Fe}(\text{CN})_6^{3-/4-}$ . The Nyquist plot exhibited a nearly-straight line for the bare GCE (Fig. 4A), which is the characteristic of a diffusion-limited electrochemical process. At the modified electrode, however, the Nyquist plots contain a clear semicircular feature in addition to the linear feature (Fig. 4B). The semicircle portions are observed at higher frequencies, and are associated with a process that is limited by electron transfer. The linear features observed at lower frequencies are attributed to diffusion-limited electron transfer [25]. The diameter of the semicircle at high frequency increases as the number of layers in the PAN-PTSA film is increased. An equivalent circuit describing this system based on the EIS shape and the reaction system is shown in Fig. 4C. The resistive component  $R_s$  is due to the sum of the electrolyte resistance and the resistance of the electrode material. The parallel elements in the circuit ( $Q_2 R_{\text{et}} Z_w$ ) are responsible for the semicircular and linear features observed in the high frequency and low frequency domains in experimental data. We obtained  $R_{\text{et}} = 3.898 \text{ k}\Omega$  when the film contained two layers, and  $R_{\text{et}} = 13.19 \text{ k}\Omega$  for PAN-PTSA films containing three layers. As a result of the increasing resistance with increasing film thickness, we conclude that PAN-PTSA acts as a blocking layer for electron and mass transfer, hindering the diffusion of ferricyanide towards the electrode surface. This behavior indicates that the PAN-PTSA film was successfully immobilized on the GC electrode surface.

Cyclic voltammetry (CV) can provide general information about the electroactivity and possible surface activity of various compounds. Cyclic voltammograms of a GC electrode modified with LB/PAN-PTSA in  $0.1 \text{ mol L}^{-1} \text{ HCl}$  solution were recorded in the potential range from  $-0.2 \text{ V}$  to  $1.2 \text{ V}$  at different scan rates. As shown in Fig. 5A, a pair of redox peaks appeared with peak potentials of  $E_{\text{pa}} = 0.669 \text{ V}$  and  $E_{\text{pc}} = 0.509 \text{ V}$  at a scan rate of  $50 \text{ mV s}^{-1}$ . This result confirmed that PAN-PTSA was successfully immobilized on the GCE surface. The anodic ( $I_{\text{pa}}$ ) and cathodic peak currents ( $I_{\text{pc}}$ ) increased with increasing scan rate. In addition, the peak currents of both the anodic and cathodic peaks were proportional to the scan rates over

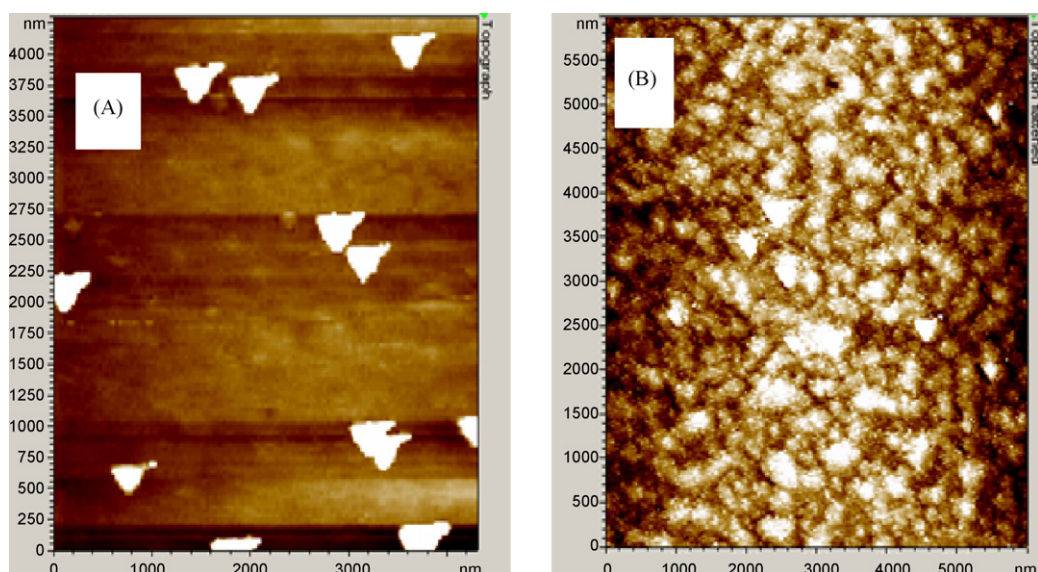
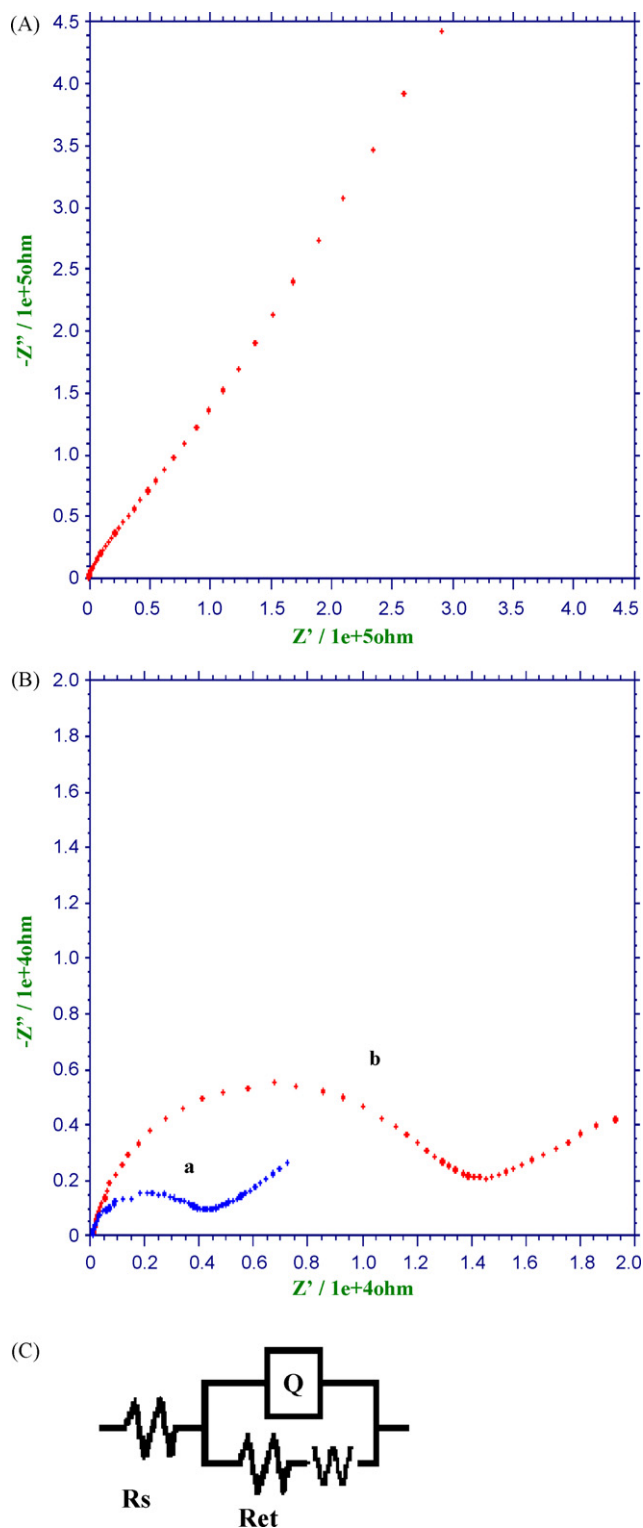


Fig. 3. AFM 2D topography image of bare monocrystalline silicon wafer (A, scan area:  $4 \mu\text{m} \times 4 \mu\text{m}$ ) and PAN-PTSA film modified silicon wafer with monolayer (B, scan area:  $6 \mu\text{m} \times 6 \mu\text{m}$ ).





**Fig. 4.** (A) Nyquist diagram of EIS at bare GCE. (B) Nyquist diagrams of EIS at two layers (a) and three layers (b) LB/PAn-PTSA/GCE. (C) Equivalent circuit. EIS condition: frequency range: 100 kHz–0.05 Hz; potential: 0.237 V; perturbation amplitude: 5 mV; solution:  $1.0 \times 10^{-3} \text{ mol L}^{-1} \text{ Fe(CN)}_6^{3-/4-}$  in  $0.2 \text{ mol L}^{-1} \text{ KCl}$ .

the range from  $10 \text{ mV s}^{-1}$  to  $100 \text{ mV s}^{-1}$  (Fig. 5B). The regression equations were:  $I_{pa}(\mu\text{A}) = -0.05784 + 0.0065v(\text{mV s}^{-1})$ ,  $r=0.991$ ;  $I_{pc}(\mu\text{A}) = -0.05394 + 0.0132v(\text{mV s}^{-1})$ ,  $r=0.996$ . The results indicated that the electrode reactions were adsorption controlled processes.

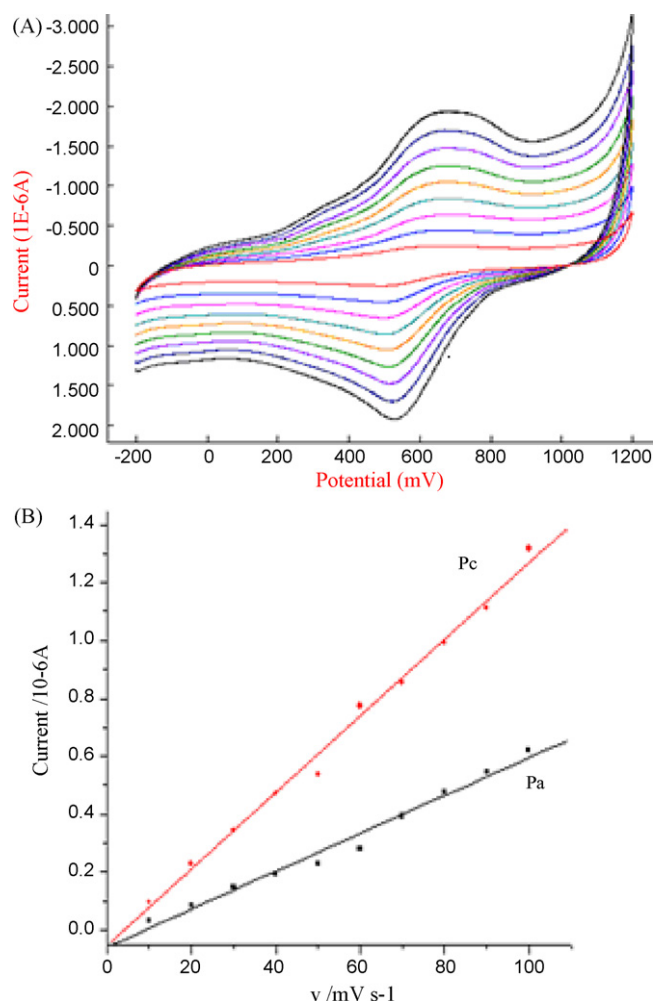


**Fig. 5.** Cyclic voltammograms of LB/PAn-PTSA/GCE (3 layers) in  $1.0 \text{ mol L}^{-1} \text{ HCl}$  with different scan rate (A), and the relationship between peak currents and scan rates (B). Scan range from inner to outer: 10, 20, 30, 40, 50, 60, 70, 80 and  $90 \text{ mV s}^{-1}$ .

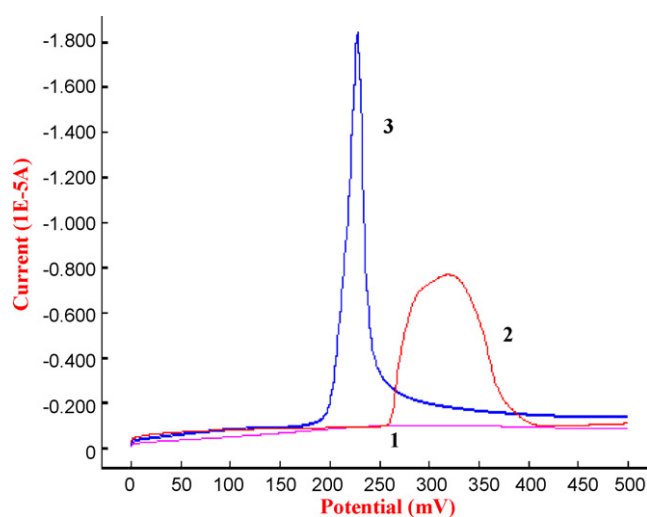


**Fig. 6.** Linear scanning stripping voltammetric curves of different electrodes in blank solution and in solution containing  $\text{Ag}^+$ . The voltammetric curve of the LB/PAn/GCE (3 layers) electrode in blank solution (curve 1); the voltammetric curves of bare GCE (curve 2) and LB/PAn/GCE (3 layers) (curve 3) electrodes in solution containing  $\text{Ag}^+$ . Blank solution:  $0.2 \text{ mol L}^{-1} \text{ KNO}_3$  (pH 5.0);  $\text{Ag}^+$  concentration:  $1.0 \times 10^{-6} \text{ mol L}^{-1}$ . Determination under optimum conditions described in Section 3.7.1.

**Table 1**

Recovery for silver in lake water and tap water samples.

Sample	Original found ( $1.0 \times 10^{-8} \text{ mol L}^{-1}$ )	Added ( $1.0 \times 10^{-8} \text{ mol L}^{-1}$ )	Found ( $1.0 \times 10^{-8} \text{ mol L}^{-1}$ )	Average recovery (%)	SD (%)
Tap water	ND	9.0	8.7	96	5.3
Lake water	ND	9.0	9.1	101	4.2

ND: no detected. Average of four determinations.

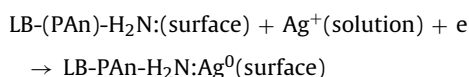
### 3.5. Electrochemical behavior of $\text{Ag}^+$ on the LB/PAn-PTSA/GCE

Linear scanning anodic stripping voltammetry was performed to study the electrochemical behavior of  $\text{Ag}^+$  on the LB/PAn-PTSA/GCE. The ability of the LB/PAn-PTSA/GCE to recognize and preconcentrate  $\text{Ag}^+$  was studied at an accumulation voltage of  $-0.56 \text{ V}$ . As shown in Fig. 6A, no peak could be discerned from  $0 \text{ V}$  to  $0.5 \text{ V}$  when the LB/PAn-PTSA/GCE was tested in blank solution (Fig. 6, curve 1). However, a sensitive anodic peak became visible at  $0.228 \text{ mV}$  when  $1.0 \times 10^{-6} \text{ mol L}^{-1} \text{ Ag}^+$  was spiked into the blank solution (Fig. 6, curve 3). The peak current was about  $18.2 \mu\text{A}$ . This indicated that the LB/PAn-PTSA/GCE was able to recognize  $\text{Ag}^+$  ions. This peak was due to the oxidation of  $\text{Ag}^0$ , which was produced by the reduction of accumulated  $\text{Ag}^+$  at  $-0.56 \text{ V}$ . This finding was consistent with the change in the  $\pi$ -A isotherm. Fig. 6 additionally contrasts the behavior of  $1.0 \times 10^{-6} \text{ mol L}^{-1} \text{ Ag}^+$  at a bare GCE (curve 2) and LB/PAn-PTSA/GCE (curve 3) under identical operating conditions.  $\text{Ag}^+$  produces a wide, level peak at a peak potential of  $\sim 0.319 \text{ V}$  at the bare GCE. When compared to the LB/PAn-PTSA/GCE, the bare GCE has lower sensitivity and worse peak shape. Based on these results, it can be deduced that the LB/PAn-PTSA film effectively coordinates to  $\text{Ag}^+$ .

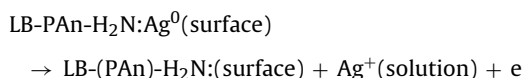
### 3.6. Mechanism of the electrode process

From the above observations, it appears that the  $\text{Ag}^+$  ion first coordinated with the N atom of PAn [26], and was then reduced to  $\text{Ag}^0$  during the preconcentration step.  $\text{Ag}^0$  was oxidized to  $\text{Ag}^+$  during the stripping step. The electrode reaction may be described as follows:

Preconcentration and reduction step:



Stripping step:



### 3.7. Analytical applications

#### 3.7.1. Optimum experimental conditions

The supporting electrolyte species and concentration, the solution pH and the accumulation potential were carefully studied during optimization, with the goal of producing the largest peak currents and best peak shape. The optimal conditions were found to be  $0.2 \text{ mol L}^{-1} \text{ KNO}_3$  (pH 5.0) as the supporting electrolyte, and  $-0.56 \text{ V}$  as the accumulation potential. The preconcentration time is known to be an important parameter in electrochemical stripping techniques, and it is known that longer accumulation times typically yield lower detection limits. At the same time, however, extended accumulation times produce narrower the linear ranges for the measurement due to electrode saturation effects. Based on the sensitivity and efficiency of the detection method, an accumulation time of  $200 \text{ s}$  was used during the following experiments.

#### 3.7.2. The relationship between peak currents and $\text{Ag}^+$ concentrations

The optimum measurement conditions were determined as to be: supporting electrolyte  $0.2 \text{ mol L}^{-1} \text{ KNO}_3$  (pH 5.0), potential range  $0$ – $0.5 \text{ V}$ , scan rate  $50 \text{ mV s}^{-1}$ , accumulation potential  $-0.56 \text{ V}$ , accumulation time  $200 \text{ s}$ . Standard solutions of  $\text{Ag}^+$  were tested in series under the optimized conditions. The peak currents were linear with  $\text{Ag}^+$  concentrations in the range from  $6 \times 10^{-10} \text{ mol L}^{-1}$  to  $1 \times 10^{-6} \text{ mol L}^{-1}$ , with the following relationship:

$$i_p(\mu\text{A}) = 0.0645 + 1.6287 \times 10^7 C \quad (r = 0.9994).$$

The detection limit was  $4.0 \times 10^{-10} \text{ mol L}^{-1}$  at an accumulation time of  $200 \text{ s}$ . The results mean that this method has a wide linear range and high sensitivity. The relative standard deviation (% R.S.D.,  $N=5$ ) for  $1 \times 10^{-6} \text{ mol L}^{-1} \text{ Ag}^+$  was  $1.56\%$ , which demonstrated the reproducibility of the method. Moreover, the LB/PAn-PTSA/GCE possesses good stability. It could be continuously used for two months, yielding a change in peak current of less than  $5\%$  for a solution with a given concentration.

#### 3.7.3. Interference studies

In order to evaluate the selectivity of the proposed method, possible interference by coexisting metal ions was studied by analyzing sample solutions containing a fixed amount of  $\text{Ag}^+$  ( $1 \times 10^{-6} \text{ mol L}^{-1}$ ) and various excess amounts of the species. The results showed that  $\text{Ti}^+$ , alkali metals and alkaline earth did not influence the height of the peak currents. However,  $15$ -fold  $\text{Cu}^{2+}$  and  $\text{Ni}^{2+}$  decreased peak currents by  $2\%$ .  $10$ -fold  $\text{Cd}^{2+}$ ,  $30$ -fold  $\text{Pb}^{2+}$  and  $58$ -fold  $\text{Co}^{2+}$  decreased peak currents by  $5\%$ . It is presumed that these metals also formed complexes with PAn, and compete with the ability of the electrode to complex  $\text{Ag}^+$  at the LB/PAn-PTSA/GCE surface. On the other hand,  $1$ -fold of  $\text{Hg}^{2+}$  was found to increase  $\text{Ag}^+$  response current. This effect can be attributed to  $\text{Hg}^{2+}$  ion reduction on the electrode, which would form a thin mercury film and increase the accumulation efficiency of  $\text{Ag}^+$ . Adding a protective reagent can eliminate the interference of above ions and markedly influence the height of the peak currents.

#### 3.7.4. Analysis of real samples

Unfortunately, suitable real sample were not found in our area. To investigate the applicability of the proposed determination method described above, tap water and lake water samples were employed to determine silver by the standard addition technique. Standard silver solutions were added to the sample solutions before analysis. The analytical results and recoveries are listed in Table 1.

### 4. Conclusions

In this work, a new electrochemical voltammetric sensor based on a GCE modified by a PAn LB film doped with p-toluenesulfonic acid was used for the detection of trace  $\text{Ag}^+$  ions. The electrochemical properties and recognition mechanism of this sensor for  $\text{Ag}^+$  in aqueous solution were discussed. Using this voltammetric sensor,  $\text{Ag}^+$  could be detected with a LOD of  $4.0 \times 10^{-10} \text{ mol L}^{-1}$  by linear scanning stripping voltammetry. This research suggests that electrodes modified with LB techniques might be a very promising means of analytical sensing.

## Acknowledgements

The financial support provided by National Natural Science Foundation of China (Nos. 20775073; 20875083) is greatly appreciated.

## References

- [1] A.G. MacDiarmid, *Angew. Chem. Int. Ed.* 40 (2001) 2581.
- [2] H.S. Kolla, S.P. Surwade, X.Y. Zhang, A.G. MacDiarmid, S.K. Manohar, *J. Am. Chem. Soc.* 127 (2005) 16770.
- [3] Z. Matharu, G. Sumana, S.K. Arya, S.P. Singh, V. Gupta, B.D. Malhotra, *Langmuir* 23 (2007) 13188.
- [4] J. Mathiyarasu, S. Senthilkumar, K.L.N. Phani, V. Yegnaraman, *J. Appl. Electrochem.* 35 (2005) 513.
- [5] V. Zucolotto, M. Ferreira, M.R. Cordeiro, C.J.L. Constantino, *Sens. Actuator B* 113 (2006) 809.
- [6] W. Yan, X.M. Feng, X.J. Chen, X.H. Li, J.J. Zhu, *Bioelectrochemistry* 72 (2008) 21.
- [7] N. Hamdi, J.J. Wang, H.G. Monbouquette, *J. Electroanal. Chem.* 581 (2005) 258.
- [8] Y.Z. Xian, F. Liu, L.J. Feng, F.H. Wu, L.W. Wang, L.T. Jin, *Electrochem. Commun.* 9 (2007) 773.
- [9] Y.J. Zou, L.X. Sun, F. Xu, *Biosens. Bioelectron.* 22 (2007) 2669.
- [10] K. Domanský, D.L. Baldwin, J.W. Grate, T.B. Hall, J. Li, M. Josowicz, J. Janata, *Anal. Chem.* 70 (1998) 473.
- [11] S. Virji, R.B. Kaner, B.H. Weiller, *Chem. Mater.* 17 (2005) 1256.
- [12] L.L. Miller, J.S. Bankers, A.J. Schmidt, D.C. Boyd, *J. Phys. Org. Chem.* 13 (2000) 808.
- [13] Z. Mandić, L. Dudić, *J. Electroanal. Chem.* 403 (1996) 133.
- [14] S. Virji, R.B. Kaner, B.H. Weiller, *J. Phys. Chem. B* 110 (2006) 22266.
- [15] S. Virji, J.X. Huang, R.B. Kaner, B.H. Weiller, *Nano Lett.* 4 (2004) 491.
- [16] J.X. Huang, S. Virji, B.H. Weiller, R.B. Kaner, *Chem. Eur. J.* 10 (2004) 1314.
- [17] M.V.B. Krishna, M. Ranjit, K. Chandrasekaran, G. Venkateswarlu, D. Karunasagar, *Talanta* 79 (2009) 1454.
- [18] G.A. Evtugyn, I.I. Stoikov, S.V. Beljyakova, R.V. Shamagsumova, E.E. Stoikova, A.Y. Zhukov, I.S. Antipin, H.C. Budnikov, *Talanta* 71 (2007) 1720.
- [19] G.A. Evtugyn, I.I. Stoikov, S.V. Beljyakova, E.E. Stoikova, R.V. Shamagsumova, A.Y. Zhukov, I.S. Antipin, H.C. Budnikov, *Talanta* 76 (2008) 441.
- [20] H. Ohnuki, T. Saiki, A. Kusakari, H. Endo, M. Ichihara, M. Izumi, *Langmuir* 23 (2007) 4675.
- [21] S. Manigandan, A. Jain, S. Majumder, S. Ganguly, K. Kargupta, *Sens. Actuator B* 133 (2008) 187.
- [22] J.H. Huang, Z.A. Wang, Q.Q. Li, K.L. Huang, S.L. Liu, *Corros. Sci. Prot. Technol.* 20 (2008) 283.
- [23] J.X. Huang, S. Virji, B.H. Weiller, R.B. Kaner, *J. Am. Chem. Soc.* 125 (2003) 314.
- [24] Y.J. Liu, F. Yin, Y.M. Long, Z.H. Zhang, S.Z. Yao, *J. Colloid Interface Sci.* 258 (2003) 75.
- [25] F. Wang, Q.Y. Liu, Y.J. Wu, B.X. Ye, *J. Electroanal. Chem.* 630 (2009) 49.
- [26] L.M. Huang, W.H. Liao, H.C. Ling, T.C. Wen, *Mater. Chem. Phys.* 116 (2009) 474.